

## Supplementary Information

### Improved photovoltaic performance of triple cation mixed-halide perovskite solar cells with binary trivalent metals incorporated on titanium dioxide electron transport layer

*M. Thambidurai<sup>1,2</sup>, Foo Shini<sup>1,2,3</sup>, K. M. Muhammed Salim<sup>2</sup>, P. C. Harikesh<sup>2</sup>, , Annalisa Bruno<sup>2</sup>, Nur Fadilah Jamaludin<sup>2</sup>, Stener Lie<sup>2</sup>, Nripan Mathews<sup>2,3</sup>, and Cuong Dang\*<sup>1,2</sup>*

- <sup>1</sup>. LUMINOUS! Centre of Excellence for Semiconductor Lighting and Displays, School of Electrical and Electronic Engineering, The Photonics Institute (TPI), Nanyang Technological University, 50 Nanyang Avenue, 639798, Singapore.
- <sup>2</sup>. Energy Research Institute @NTU (ERI@N), Research Techno Plaza, X-Frontier Block, Level 5, 50 Nanyang Drive, 637553, Singapore.
- <sup>3</sup>. School of Materials Science and Engineering, Nanyang Technological University, 50 Nanyang Avenue, 639798, Singapore.

\*Email: hcdang@ntu.edu.sg

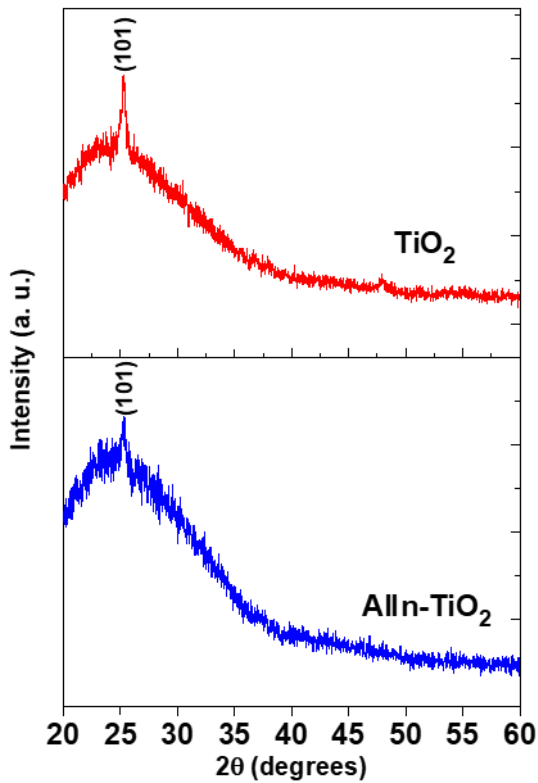


**Figure S1.** X-ray diffraction patterns of TiO<sub>2</sub> and AlIn-TiO<sub>2</sub> films.

From the cross sectional SEM images, there was negligible difference in thickness of both pristine TiO<sub>2</sub> and AlInTiO<sub>2</sub> films, whereby both films had similar thicknesses of 60 nm. Such low doping concentration in our doped film makes no impact on the film formation in our spin-casting technique. As such, the decrease in peak intensity is probably due to the presence of dopant in our film.

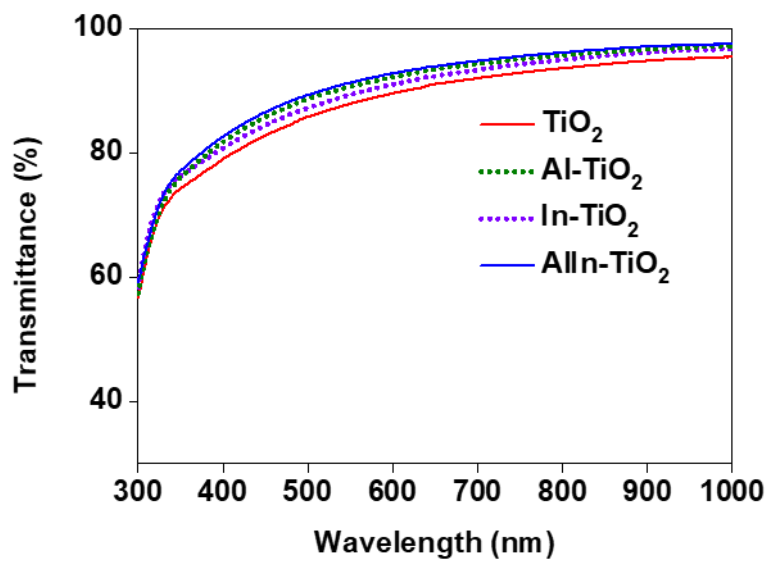


**Figure S2.** Transmittance spectra of  $\text{TiO}_2$ ,  $\text{Al-TiO}_2$ ,  $\text{In-TiO}_2$  and  $\text{AlIn-TiO}_2$  films.

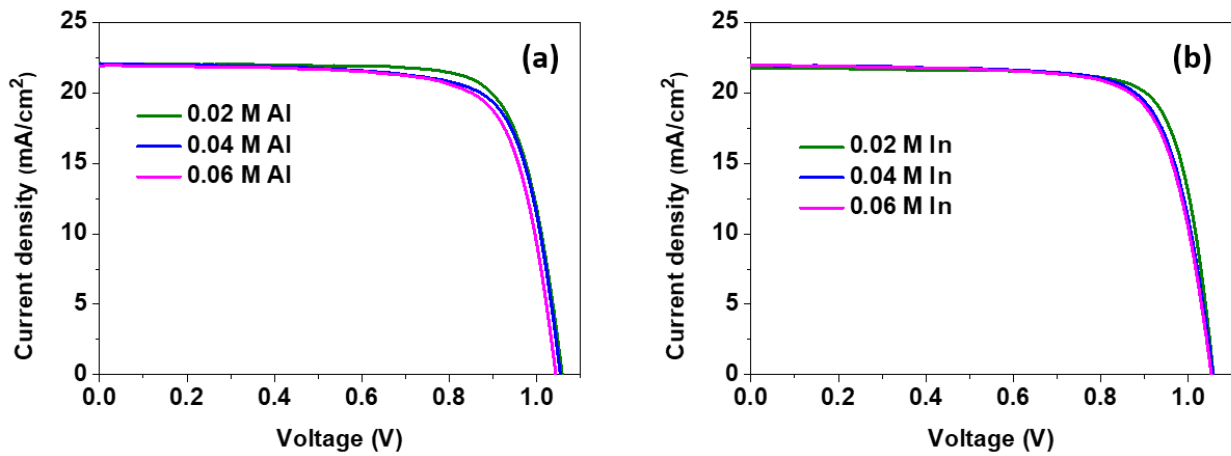


**Figure S3.** Current density-voltage (J-V) characteristics of perovskite solar cells with Al-TiO<sub>2</sub> and In-TiO<sub>2</sub> ETLs.

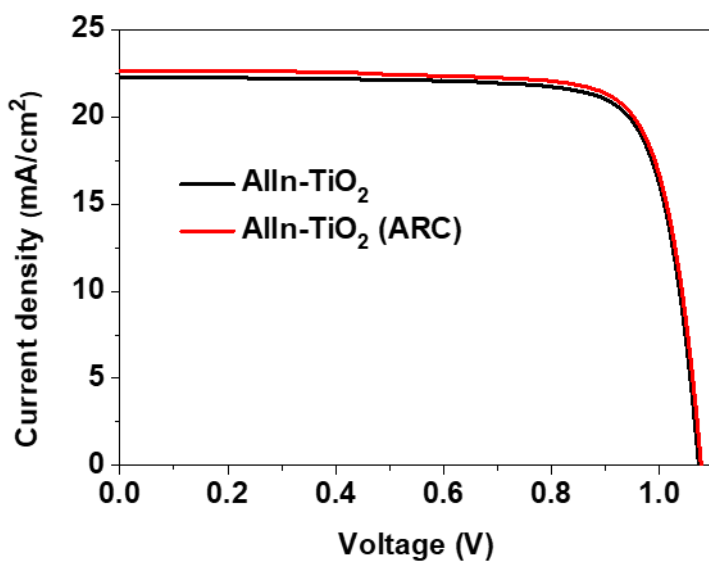


**Figure S4.** Current density-voltage (J-V) characteristics of AlIn-TiO<sub>2</sub> based perovskite solar cells with and without anti-reflection film (ARC).

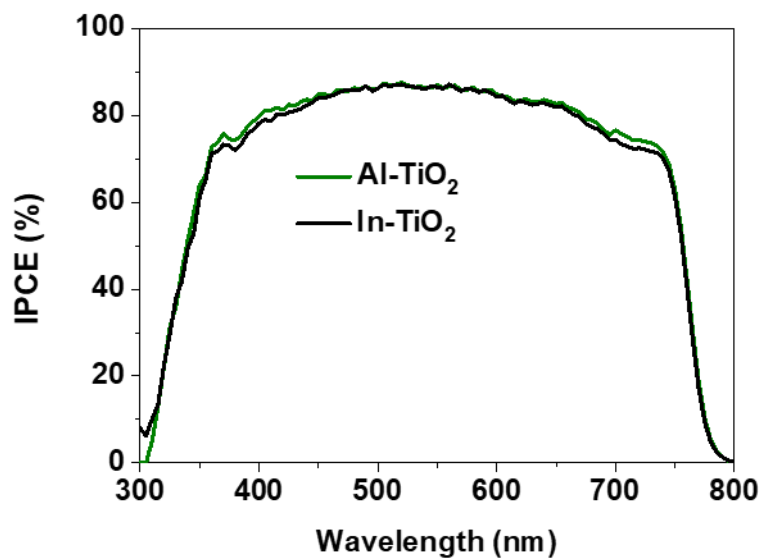


**Figure S5.** IPCE spectra of perovskite solar cells with Al-TiO<sub>2</sub> and In-TiO<sub>2</sub>.

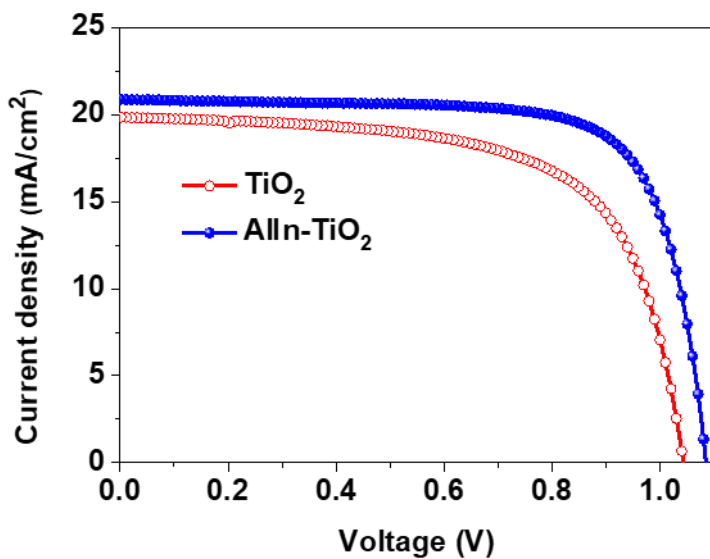


**Figure S6.** Current density-voltage (J-V) curves of the  $\text{TiO}_2$  and  $\text{AlIn-TiO}_2$  based perovskite solar cells after 25 days in ambient condition.

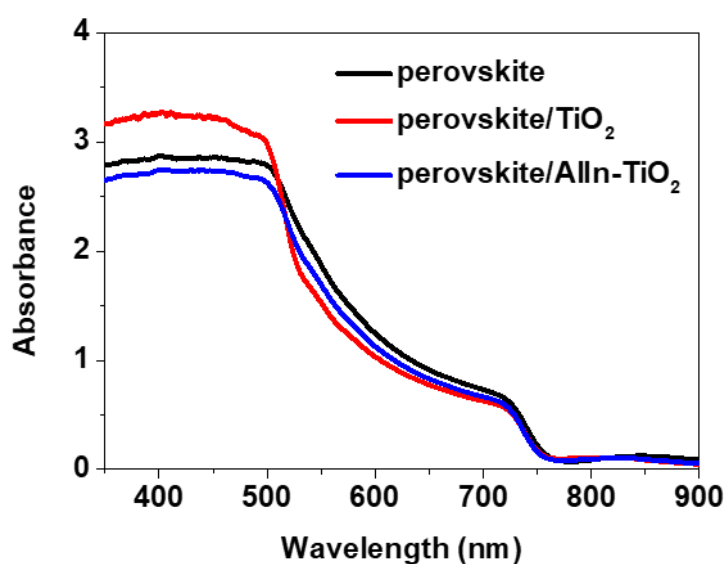


**Figure S7.** Absorption spectra of perovskite coated TiO<sub>2</sub> and AlIn-TiO<sub>2</sub> films.

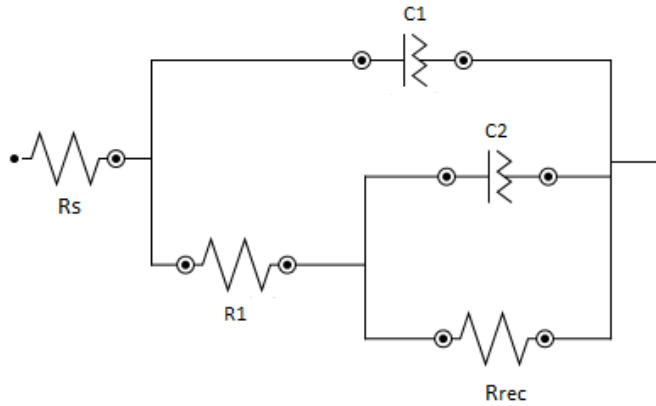


**Figure S8.** Equivalent circuit for the analysis of perovskite solar cells.

To gain more insight into the charge transport and recombination dynamics in the devices, EIS measurements were carried out for the  $\text{TiO}_2$  and  $\text{AlIn}-\text{TiO}_2$  based devices under dark in the Ar atmosphere (glove box). The impedance spectra exhibited two arcs in the complex impedance plot as reported widely in literature for devices with good charge extraction. The data was analysed using the commonly reported [1-2] equivalent circuit consisting of a series resistance ( $R_s$ ), two capacitive ( $C_1$  and  $C_2$ ) and two resistive components ( $R_{rec}$  and  $R_1$ ). The series resistance arises from the Ohmic contribution from wires and contacts. Capacitance  $C_1$  related to the high frequency part of the spectra originates from the dielectric bulk capacitance of the device and the low frequency capacitance  $C_2$  is generally associated with the trapping and detrapping of carriers. The origin of the resistances  $R_1$  and  $R_{rec}$  are not clearly established but they are often associated with the bulk conductivity and recombination resistance of the device.

**Table S1:** Photovoltaic parameters of perovskite solar cells with Al-TiO<sub>2</sub> and In-TiO<sub>2</sub>.

<b>ETLs</b>	<b>V<sub>oc</sub></b> <b>[V]</b>	<b>J<sub>sc</sub></b> <b>[mA cm<sup>-2</sup>]</b>	<b>FF</b> <b>[%]</b>	<b>PCE</b> <b>[%]</b>
0.04 M Al-doped TiO <sub>2</sub>	1.05	22.04	75.26	17.43
0.06M Al-doped TiO <sub>2</sub>	1.04	22.02	74.93	17.15
0.04 M In-doped TiO <sub>2</sub>	1.05	21.94	75.89	17.57
0.06 M In-doped TiO <sub>2</sub>	1.05	21.98	75.02	17.33

**Table S2:** The Hall effect parameters of TiO<sub>2</sub> and AlIn-TiO<sub>2</sub> devices, with structure of glass/TiO<sub>2</sub> (or AlIn-TiO<sub>2</sub>)/Au.

ETLs	Type	Hall mobility (cm V <sup>-1</sup> S <sup>-1</sup> )	Carrier density (1/cm <sup>3</sup> )	Resistivity (Ohm*cm)	Conductivity (S cm <sup>-1</sup> )
TiO <sub>2</sub>	N	1.03	$2.14 \times 10^{14}$	28310	$3.53 \times 10^{-5}$
AlIn-TiO <sub>2</sub>	N	1.15	$2.85 \times 10^{14}$	18926	$5.28 \times 10^{-5}$

**Table S3:** Analysis of the TRPL with two-exponential decay characteristics for perovskite, perovskite/TiO<sub>2</sub> and perovskite/AlIn-TiO<sub>2</sub>.

Samples	A <sub>1</sub>	τ <sub>1</sub> (ns)	A <sub>2</sub>	τ <sub>2</sub> (ns)	τ average (ns)
Perovskite	0.25	8.47	0.75	309.1	233.9
Perovskite /TiO <sub>2</sub>	0.20	9.10	0.80	258.4	208.5
Perovskite /AlIn- TiO <sub>2</sub>	0.32	10.6	0.68	215.7	150.1

**Table S4:** The fitted parameters for EIS measurements acquired under dark condition.

ETLs	$R_{\text{series}} (\Omega)$	$R_{\text{rec}} (K\Omega)$
TiO <sub>2</sub>	19.5	5.40
AlIn- TiO <sub>2</sub>	18.7	56.9

## References

- [1] A. Guerrero, G. G.-Belmonte, I. M.-Sero, J. Bisquert, Y. S. Kang, T. J. Jacobsson||, J.-P. C.-Baena, A. Hagfeldt, *J. Phys. Chem. C* **2016**, *120*, 8023.
- [2] I. Zarazua, G. Han, P. P. Boix , S. Mhaisalkar, F. F.-Santiago, I. M.-Seró , J. Bisquert, G. G.-Belmonte, *J. Phys. Chem. Lett.* **2016**, *7*, 5105.